NAA-SR-2557
COPY

THE CALCULATION OF GAMMA-RAY HEATING IN TARGET SAMPLES LOCATED IN THE BSR SHIELD

AEC Research and Development Report

ATOMICS INTERNATIONAL
A DIVISION OF NORTH AMERICAN AVIATION, INC.

NAA-SR-2557
PHYSICS AND MATHEMATICS
36 PAGES

THE CALCULATION OF GAMMA-RAY HEATING IN TARGET SAMPLES LOCATED IN THE BSR SHIELD

BY

D. S. DUNCAN

ATOMICS INTERNATIONAL

A DIVISION OF NORTH AMERICAN AVIATION, INC.
P.O. BOX 309 CANOGA PARK, CALIFORNIA

CONTRACT: AT(11-1)-GEN-8
ISSUED: NOVEMBER 1, 1958

DISTRIBUTION

This report has been distributed according to the category "Physics and Mathematics" as given in "Standard Distribution Lists for Unclassified Scientific and Technical Reports" TID-4500 (13th Ed., Rev.), February 15, 1958. A total of 650 copies was printed.

TABLE OF CONTENTS

		Page No.
	Abstract	5
I.	Introduction	7
II.	Definition of Terms	7
III.	Experimental Procedure	9
IV.	Description of the Reactor Core	10
V.	Core Gamma-Ray Spectrum	11
	A. Gamma Rays from the Reaction $U^{235}(n, f)$	11
	B. Gamma Rays from the Reaction $U^{235}(n, \gamma)$	12
	C. Capture Gamma Rays from Hydrogen and Aluminum	13
	D. Decay Gamma Rays from Al^{28}	13
	E. Gamma Rays from Fission Products	13
VI.	Description of the Attenuation of Source Radiations	16
	A. Core Radiations	16
	B. Shield Capture Gamma Rays	17
	C. Target Capture Gamma Rays	21
	D. Target Decay Beta Particles	23
VII.	Absorption Coefficients and Buildup Factors	23
VIII.	Results	25
IX.	Conclusion	27
	References	28

LIST OF TABLES

I.	BSR Core Gamma-Ray Source Strength	15
II.	Capture Gamma-Ray Spectrum Used for Target Materials	22
III.	Calculated and Measured Heat Generation Rates	26

LIST OF FIGURES

Page No.

1. Thermal Neutron Flux in BSR Water Shield for Loading 33 . . 30
2. Geometry for Uniform Cylindrical Source With Slab Shield . . 31
3. Geometry for Exponential Slab Source with Slab Shield. . . . 31
4. Electron Cross Section for BSR Core 32
5. Linear Absorption Coefficient for BSR Core 33
6. Gamma-Ray Heating in Aluminum Target 34
7. Gamma-Ray Heating in Iron Target 35
8. Gamma-Ray Heating in Lead Target 36

ABSTRACT

An analysis has been made of gamma-ray heating in lead, iron, and aluminum samples as a function of position in the water shield surrounding the BSR core. The results obtained are in excellent agreement with experimental measurements. The average values of the calculated gamma-ray heat generation rates in the target materials were found to agree with the measured values, over the range of distances from the core for which the measurements were made, to within 4 per cent, with a maximum deviation of 20 per cent. The analysis includes the evaluation of the heat generation rates in the samples from core gamma rays, shield capture gamma rays, target capture gamma rays, and target decay beta particles. The methods of evaluation and the assumptions necessary are discussed. It is concluded that the basic gamma-ray data and calculational methods employed may be used in similar analyses for other reactor systems.

I. INTRODUCTION

One of the many problems encountered in the design of reactor systems is to determine the heat generation rates and resultant thermal stresses caused by the absorption of gamma-rays and neutrons in the structural materials outside of the core. A rigorous analysis of this problem is, in general, almost prohibitive due to the computational difficulties involved in a direct numerical integration of the Boltzmann equation. Consequently, a number of simplifying assumptions regarding source-spectrum, geometry, and gamma-ray behavior must be made. The purpose of this report is to assess the adequacy of the assumptions made in the methods presently being employed in the design of the Organic Moderated Reactor (OMR). This is accomplished by comparing calculated heat generation rates with experimentally measured values.

Gamma-ray heating has been measured in lead, iron, and aluminum samples located in the water shield surrounding the Bulk Shielding Reactor (BSR). Since this reactor is quite similar in design to the OMR, these measurements are used in comparing caluclated heat generation rates with experiment.

The results of the aforementioned gamma-ray heating measurements are shown in Table III. Analyses of these data by Bertini, et al.[4] and French[30] have shown excellent agreement between experiment and theory; however, their methods of analysis differ considerably from those presented here. The methods described in this report are quite similar to those reported in NAA-SR-1921,[2] in which an analysis of the gamma-ray dose rate in the BSR shield is described. For completeness and clarity of presentation, some of the applicable information from this earlier report is repeated here in Sections IV through VI. A., inclusive. A complete description of the heat generation rate analysis and the results obtained are presented in the following sections.

II. DEFINITION OF TERMS

$\phi_n(x)$ = thermal neutron flux in shield region (n/cm^2-sec)

$\bar{\phi}_{th}$ = average thermal neutron flux in the core (n/cm^2-sec)

P = reactor power level (Mw)

N_o = Avogadro's number

σ_f = U^{235} fission cross section corrected to 63° C and for a Maxwellian distribution (cm^2)

M = mass of U^{235} (kg)

H = heat generation rate (watts/gm)

S_v = gamma-ray source strength (Mev/cc-sec)

B_a = energy absorption buildup factor

$\frac{\mu_e}{\rho}$ = energy mass absorption coefficient (cm^2/gm)

μ_i = linear absorption coefficient in the i^{th} absorbing medium (cm^{-1})

μ_s = linear absorption coefficient in the core (cm^{-1})

μ_t = linear absorption coefficient of shield region containing source (cm^{-1})

r_i = distance traveled in the i^{th} absorbing medium (cm)

a_i = thickness of the i^{th} shield region (cm)

t = thickness of shield region containing source (cm)

z = effective self-attenuation distance (cm)

R = distance from surface of cylinder to detector (cm)

R_o = radius of cylindrical or spherical source region (cm)

h = height of cylindrical source (cm)

$$\mu r = \sum_i \mu_i r_i$$

$$\mu a = \sum_i \mu_i a_i$$

$$p = \mu_t t + \mu a$$

$b = \mu_s z + \mu a$

$\varkappa_t$ = reciprocal of thermal neutron relaxation length (cm^{-1})

$\beta = \frac{\varkappa_t}{\mu_t}$

A, α, C_1, C_2 = constants used for the analytical representations of the buildup factor

k = factor converting Mev/sec to watts = 1.60×10^{-13} watts/$\frac{\text{Mev}}{\text{sec}}$

Σ_a = macroscopic thermal neutron absorption cross section in the region t (cm^{-1})

η = number of gamma rays of a given energy (or within a given energy interval) created per neutron capture

E_γ = energy of capture gamma ray being considered (Mev)

$\theta = \tan^{-1} \frac{h}{2(R+z)}$

$$F[\theta, b(1-\alpha)] = \int_o^\theta e^{-b(1-\alpha)\sec w}\, dw$$

$$E_1(y) = \int_1^\infty \frac{e^{-yt}}{t}\, dt$$

$$f_o(y) = \frac{e^{-y}}{E_1(y)} - y.$$

III. EXPERIMENTAL PROCEDURE

Because the purpose of this study is to compare results obtained from a calculational method with those obtained experimentally, a brief description of the experimental procedure is given.[1] Heat generation rates were measured in iron, aluminum, and lead samples located in the water shield surrounding the BSR core. The three target samples were cylindrical in shape, having a diameter and height equal to three-eighths of an inch and 2 inches, respectively. The samples were

placed in 1-inch diameter capsules and positioned along the horizontal centerline of the core at distances of 0 to 9 inches from the core face. The change in the temperature of the samples as a function of time was measured by means of thermocouples embedded in the target materials. From the observed temperature changes, the heat generation rates in the samples were determined. The results obtained are shown in Table III and in Fig. 6, 7 and 8.

IV. DESCRIPTION OF THE REACTOR CORE

The design of the Bulk Shielding Reactor has been described elsewhere[3] and will not be elaborated on here. The core of the reactor in which the measurements were made[1] contained 28 fuel elements with a total of 3.6 kg of U^{235}. In the analysis which follows, the metal-to-water volume ratio in the core was taken to be 0.70. From this, it was found that the core contained 5.84×10^4 gm of water, 3.84×10^3 gm of uranium ($U^{235} + U^{238}$), and 1.096×10^5 gm of aluminum. The total volume of the core was taken to be 9.92×10^4 cm^3.

The average thermal neutron flux in the uranium was calculated using the expression

$$\bar{\phi}_{th} = \frac{3.1 \times 10^{16} P}{\frac{N_o}{235} \times 10^3 \sigma_f M} \quad . \qquad \ldots(1)$$

With $\sigma_f = 478 \times 10^{-24} cm^2$, one obtains $\bar{\phi}_{th} = 7.02 \times 10^{12}$ $\frac{\text{neutrons}}{cm^2\text{-sec-Mw}}$.

This is actually the average thermal neutron flux in the uranium, and not in the reactor. However, for the particular reactor under consideration, it is not expected that the core averaged thermal neutron flux will vary significantly from this value. As a result, this value shall be used to represent the average thermal neutron flux in the core.

In most of the practical problems of shield design and heat generation, the details of the power distribution in the core are not known. Consequently, some assumption relating to this distribution must be made. The one which is the simplest and probably the most often used is that the power distribution in the core is uniform. This assumption is used in the analysis which follows.

V. CORE GAMMA-RAY SPECTRUM

The sources of core gamma radiation considered in this analysis include the gamma rays generated in the following reactions: $U^{235}(n,f)$, $U^{235}(n,\gamma)$, $H(n,\gamma)$, $Al^{27}(n,\gamma)$, and $Al^{28} \rightarrow \gamma + \beta$, as well as those emitted by fission products. Gamma rays from inelastic scattering in aluminum[4] and uranium,[5] as well as capture gamma rays from U^{238}, are not considered because of their relatively low intensities. In low-enriched systems, uranium inelastic gammas and U^{238} capture gammas should be included. The spectra generated from each of the reactions considered are discussed below.

A. GAMMA RAYS FROM THE REACTION $U^{235}(n,f)$

Until recently there has been some question concerning the spectrum from prompt fission gamma rays. Two early measurements[6,7] appear to agree in the total energy available, but not in the average energy per photon. The data of Deutsch and Rotblat[7] gives a total energy of 5.1 ± 0.3 Mev/fission and an average energy per photon of 1 Mev; whereas, Kinsey et al., give 4.6 ± 0.1 Mev/fission, and an average energy of 2.5 Mev. Another measurement,[8] reported at the Reactor Shielding Information Meeting in November, 1953, indicated a very pronounced peak at about 1 Mev, with not other strong lines appearing. A still more recent measurement was reported by Gamble[9] at Oak Ridge National Laboratory in June , 1955. From a curve of Gamble's data, which plots photons/fission-100 Kev as a function of gamma-ray energy over the range from 0 to 7.6 Mev, the spectrum of prompt fission gamma rays can be approximated[5] by

$$N_u'(E) = 7.6e^{-1.01E} \text{ photons/Mev-fission} \quad . \qquad \ldots(2)$$

The total energy released per fission and the average energy per photon are obtained as follows:

$$E_T = \int_0^{7.6} EN_u'(E)dE = 7.45 \text{ Mev/fission} \quad , \qquad \ldots(3)$$

$$\bar{E} = \frac{\int_o^{7.6} EN_u'(E)dE}{\int_o^{7.6} N_u'(E)dE} = \frac{7.45}{7.52} = 0.991 \; Mev/photon. \qquad \ldots(4)$$

Although the average photon energy (Eq. 4) appears to be in good agreement with previously reported measurements,[7,8] the total energy released per fission (Eq. 3) is considerably higher. However, preliminary data from measurements made at Oak Ridge National Laboratory by Maienschein, Peele, and Love[10] tend to substantiate the total energy released per fission reported by Gamble. Consequently, it was decided to use the spectrum defined by Eq. (2) in this analysis.

B. GAMMA RAYS FROM THE REACTION $U^{235}(n,\gamma)$

When U^{235} captures a neutron producing U^{236}, the excess energy (neutron binding energy) is emitted in the form of gamma rays. The neutron binding energy for this reaction is 6.426 Mev.[11] Very little information is available concerning the spectrum of this radiation; it has been conjectured,[5] however, that the radiation has the same spectral distribution as that of the prompt fission gamma rays. For lack of better information, this assumption is used in this analysis.

Because the BSR is a thermal reactor, the ratio of the number of radiative captures to the number of fissions in U^{235} is assumed to be equal[12] to 0.184. Thus, the spectrum from radiative capture can be approximated[5] by

$$N_u''(E) = 1.21e^{-1.01E} \; photons/Mev\text{–}fission. \qquad \ldots(5)$$

Therefore, the spectrum of prompt fission gamma rays plus U^{235} capture gamma rays is, by addition

$$N_u(E) = 8.81e^{-1.01E} photons/Mev\text{–}fission., \qquad \ldots(6)$$

and, the total gamma-ray energy released per fission by U^{235} within discrete energy intervals is

$$E_{ab} = 8.81 \int_a^b E\, e^{-1.01E} dE \; Mev/fission \; . \qquad ...(7)$$

C. CAPTURE GAMMA RAYS FROM HYDROGEN AND ALUMINUM

The capture gamma-ray spectrum from hydrogen is well known to be composed of a single line at 2.23 Mev, one photon being emitted per neutron capture.[13] Detailed information on the capture gamma-ray spectrum from aluminum in the region above 2.7 Mev has been obtained by Kinsey and co-workers.[14] The capture gamma-ray spectrum from aluminum in the region below 2.7 Mev has been obtained by Braid.[17]

D. DECAY GAMMA RAYS FROM Al^{28}

When aluminum absorbs a neutron, the result is Al^{28}, which has a half-life of 2.27 minutes.[18] This isotope decays by emission of a 2.87 Mev beta particle and a 1.78 Mev gamma ray.[18] Because the half-life is so short, it may safely be assumed that when the BSR measurements were taken, the Al^{28} activity in the core was effectively saturated. Thus, the 1.78 Mev gamma ray was included in the analysis.

E. GAMMA RAYS FROM FISSION PRODUCTS

The fission product decay gamma-ray spectrum between 0.36 and 5.8 Mev reported by Peele, Zobel, and Love[19] has been approximated[5] by

$$N_p(E) = 9.0\, e^{-1.33E} \; photons/Mev\text{-}fission \; . \qquad ...(8)$$

Thus, the total fission product gamma-ray energy released per fission by U^{235} within discrete energy intervals is (refer to next page):

$$E_{ab} = 9.0 \int_a^b E\, e^{-1.33E}\, dE \ \text{Mev/fission.} \qquad \ldots(9)$$

The spectrum given by Eq. (8) was based upon a fuel irradiation time of approximately 1 hour, so that the decay gamma-ray activity of the long-lived fission products, i.e., those with half-lives greater than several hours, was not considered. Bertini, et al.[5], has shown that even though there exists an estimated probable error of ± 20 per cent in this spectrum, it is still in close agreement with the spectrum estimated by Way[20] after correcting the latter for the contribution from long-lived fission products.

For the purpose of finding the BSR core gamma-ray source strength, the aluminum capture gamma-ray spectrum was divided into eleven energy intervals with a single representative energy chosen for each. Because the total energy accounted for by Kinsey and by Braid was 7.8 Mev, the gamma-ray energy released per thermal neutron capture within each interval was obtained by summing up the individual contribution in each interval and normalizing so that the total energy per capture would be equal to the neutron binding energy (7.72 Mev).

The gamma-ray energy spectrum for the U^{235} (n,f) and U^{235} (n,γ) reactions, Eq. (6), was integrated over discrete energy intervals ranging from zero to 10 Mev, and the gamma-ray energy spectrum for the fission products, Eq. (8), was integrated over intervals ranging from 0.36 to 5.8 Mev. Wherever possible, these intervals were chosen so that their average energies would correspond to the specific energies used to represent the aluminum capture gamma-ray spectrum. By so doing and by including the hydrogen capture and aluminum decay gamma rays, it was possible to represent the entire gamma-ray energy spectrum of the core (over the range of energies considered) by 18 discrete energy lines with fairly uniform spacing. The result of the calculations for determining the gamma-ray source strength of the core, using these energy lines, is summarized in Table I.

TABLE I

BSR CORE GAMMA-RAY SOURCE STRENGTH

Gamma-Ray Energy (Mev)	Source Strength $\frac{\text{Mev} \times 10^{-5}}{\text{cc-sec-watt}}$					
	U^{235}(n, f and n, γ)	Al(n, γ)	H(n, γ)	$Al^{28} \rightarrow \gamma$	Fission Products	Total
0.30	3.34	-	-	-	-	3.34
0.43	-	-	-	-	1.68	1.68
1.00	7.80	0.0311	-	-	5.80	13.63
1.80	6.41	-	-	0.588	3.73	10.73
2.23	-	-	1.86	-	-	1.86
2.40	2.35	0.189	-	-	1.11	3.65
3.00	3.22	0.395	-	-	1.28	4.89
3.70	1.47	0.213	-	-	0.463	2.14
4.25	0.805	0.272	-	-	0.212	1.29
4.75	0.706	0.242	-	-	0.122	1.07
5.20	0.138	0.892	-	-	0.0585	0.286
5.60	0.217	0.150	-	-	0.0370	0.404
6.20	0.265	0.107	-	-	-	0.372
6.80	0.0784	0.0620	-	-	-	0.140
7.20	0.0553	-	-	-	-	0.0553
7.72	0.0540	0.866	-	-	-	0.925
8.50	0.0451	-	-	-	-	0.0451
9.50	0.0184	-	-	-	-	0.0184

VI. DESCRIPTION OF THE ATTENUATION OF SOURCE RADIATIONS

A. CORE RADIATIONS

The heat generation rate at any position in the shield caused by gamma radiation from the core may be described by the expression

$$H = \frac{\mu_e}{\rho} k \int_V \frac{S_v B_a e^{-\mu r}}{4\pi r^2} dV \quad . \qquad \ldots(10)$$

Let us consider the BSR core as a uniform homogeneous volume-equivalent right-circular cylinder viewed from the side with the radius and height equal to 21.5 cm and 61.0 cm, respectively. The source geometry is shown in Fig. 2. It has been shown[21] that a source of this geometry may be approximated by a line source having an intensity per unit length equal to

$$S_L = \pi R_o^2 S_v \qquad \ldots(11)$$

provided that the line source is placed within the cylinder so as to correctly account for the self-absorption of the cylinder. Thus, Eq. (10) may be written as

$$H = \frac{\mu_e k}{\rho} \int_L \frac{R_o^2 S_v B_a \exp\left[-(\mu_s z + \mu a) \sec\psi\right]}{4\pi[(z+a) \sec\psi]^2} dL \qquad \ldots(12)$$

Representing the energy absorption buildup factor by the expression

$$B_a(\mu r) = A e^{\alpha(\mu r)}$$

and substituting

$$dL = (R + z) \sec^2\psi d\psi$$

Eq. (12) becomes

$$H = \frac{\mu_e k}{\rho} \int_{\theta_1}^{\theta_2} \frac{R_o^2 S_v A \exp\left[-(\mu_s z + \mu a)(1-\alpha) \sec \psi\right]}{4(R+z)} \, d\psi \qquad \ldots(13)$$

or, when $\theta = -\theta_1 = \theta_2$

$$H = \frac{\mu_e k A S_v R_o^2}{2\rho(a+z)} F[\theta, b(1-\alpha)] \ watts/gram. \qquad \ldots(14)$$

Using the curves obtained by Foderaro and Obenshain[21] from an empirical fit to the exact calculations by Taylor and Obenshain,[22] the approximate location of the equivalent line source, i.e., the value of z, may be easily determined.

The values for A and α must be determined each time Eq. (14) is evaluated, i.e., each time the energy or shield thickness is changed. This is most easily accomplished by using a semi-logarithmic plot of the energy absorption buildup factor as a function of the penetration, in mean free paths, to graphically obtain the best fit to B_a in the region of concern. By carefully choosing the values for A and α which give the best fit to the buildup factor data over an interval from b to $(b + x)$, where $x \geq 3$ mean free paths, excellent agreement to an exact representation of the data may be obtained.

The contribution made by the core radiations to the heat generation rates in the target materials was thus evaluated by using Eq. (14). Because of the small amount of penetration of the core radiation in the water shield, the energy absorption buildup factor for the core material was used in the calculation.

B. SHIELD CAPTURE GAMMA RAYS

The heat generation rate at a position P (see Fig. 3) in the shield caused by capture gamma rays produced in any shield region t is described by the expression

$$H = \frac{\mu_e k}{\rho} \int_{V_t} \frac{\phi_n(x) \Sigma_a \eta E_\gamma B_a(\mu r) \, e^{-\mu r}}{4\pi r^2} \, dV_t. \qquad \ldots(15)$$

Using the notation in Fig. 3, Eq. (15) may be rewritten in slab geometry as

$$H(slab) = \frac{\mu_e k \Sigma_a \eta E_\gamma}{2\rho} \int_t^o \phi_n(x)dx \int_o^{\pi/2} B_a \exp\left[-\frac{\mu a + \mu_t t - \mu_t x}{\cos\theta}\right] \tan\theta d\theta \quad \ldots(16)$$

This expression is essentially an integration over a series of infinite plane sources of thickness dx. Because this source is more appropriately represented by an infinite cylinder than by an infinite slab, the well-known transformation from an infinite plane source to a cylindrical shell source[23] will be used and the integration carried out over the shells. Thus, referring again to Fig. 3,

$$H(cylindrical\ shell) = \left[\frac{R_o + a_o + x}{R_o + R}\right]^{1/2} H(plane) \quad \ldots(17)$$

which, when substituted into Eq. (16) gives

$$H(cylinder) = \frac{\mu_e k \Sigma_a \eta E_\gamma}{2\rho} \int_t^o \left[\frac{R_o + a_o + x}{R_o + R}\right]^{1/2} \phi_n(x)\,dx$$

$$\cdot \int_o^{\pi/2} B_a \exp\left[-\left(\frac{\mu a + \mu_t t - \mu_t x}{\cos\theta}\right)\right] \tan\theta d\theta . \quad \ldots(18)$$

In order to simplify the integration, the experimentally measured thermal neutron flux,[24,25] shown graphically in Fig. 1, was replotted by multiplying ϕ_n (measured) by the ratio

$$\left[\frac{R_o + a_o + x}{R_o + R}\right]^{1/2} .$$

The resultant curve was then represented by a series of exponentials, such that in the region t

$$\left[\frac{R_o + a_o + x}{R_o + R}\right]^{1/2} \phi_n(x) \cong \phi_n'(0)\, e^{-\mathcal{K}_t x} , \qquad \ldots(19)$$

where

$$\phi_n'(0) = \left[\frac{R_o + a_o}{R_o + R}\right]^{1/2} \phi_n(0)$$

and $\mathcal{K}_t$ is a constant chosen so as to give the best fit to the replotted flux in the region t. Substituting Eq. (19) into Eq. (18)

$$H = \frac{\mu_e k \Sigma_a \eta E_\gamma \phi_n'(0)}{2\rho} \int_t^0 e^{-\mathcal{K}_t x}\, dx \int_0^{\pi/2} B_a \exp\left[-\frac{\mu a + \mu_t t - \mu_t x}{\cos\theta}\right] \tan\theta d\theta . \qquad \ldots(20)$$

For a geometry such as this, it has been found[26] that a polynomial type representation to the buildup factor will lead to an exact solution. Replacing B_a in Eq. (20) by a quadratic of the form

$$B_a(\mu r) = 1 + C_1 \mu r + C_2 \mu^2 r^2$$

and integrating the resulting expression, the heat generation rate becomes

$$H = \frac{\mu_e k \phi_n'(0) \Sigma_a \eta E_\gamma e^{-\mathcal{K}_t t}}{2\rho \mathcal{H}_t} \left\{ e^{\mathcal{K}_t t} E_1(\mu_t t + \mu a) - E_1(\mu a) \right.$$

$$\left. + e^{-\frac{\mathcal{K}_t}{\mu_t}\mu a} \left[E_1\left[\left(1 - \frac{\mathcal{K}_t}{\mu_t}\right)\mu a\right] - E_1\left[\left(1 - \frac{\mathcal{K}_t}{\mu_t}\right)(\mu_t t + \mu a)\right]\right]\right.$$

$$+ C_1 \frac{\mathscr{L}_t}{\mathscr{K}_t - \mu_t} e^{\mathscr{K}_t t - \mu a} \left[e^{-\mu_t t} - e^{-\mathscr{K}_t t} \right]$$

$$+ C_2 \frac{\mathscr{K}_t}{\mathscr{K}_t - \mu_t} e^{\mathscr{K}_t t - \mu a} \left[\mu_t t\, e^{-\mu_t t} + \left(\mu a + \frac{\mathscr{K}_t - 2\mu_t}{\mathscr{K}_t - \mu_t} \right) \left(e^{-\mu_t t} - e^{-\mathscr{K}_t t} \right) \right] \Bigg\} . \quad \ldots(21)$$

$E_1(y)$ can be calculated by means of the formula

$$E_n(y) = \frac{e^{-y}}{y + n - 1 + f_{n-1}(y)} \quad \ldots(22)$$

where f_n (y) may be obtained from the curves given in NAA-SR-1921.[2]

Substituting Eq. (22) into Eq. (21) and rearranging the terms,

$$H = \frac{\mu_e k \phi_n'(0) \Sigma_\cdot \eta E_\gamma e^{-p}}{2\rho \mathscr{K}_t} \left\{ \frac{1}{p + f_o(p)} - \frac{1}{(1-\beta)p + f_o[(1-\beta)p]} \right.$$

$$+ \frac{\beta}{\beta - 1} \left[C_1 + C_2 \left(p + \frac{\beta - 2}{\beta - 1} \right) \right] + e^{(1-\beta)\mu_t t} \left[\frac{1}{(1-\beta)\mu a + f_o[(1-\beta)\mu a]} \right.$$

$$\left. \left. - \frac{1}{\mu a + f_o(\mu a)} - \frac{\beta}{\beta - 1} \left[C_1 + C_2 \left(\mu a + \frac{\beta - 2}{\beta - 1} \right) \right] \right] \right\} . \quad \ldots(23)$$

Similarly, it can be shown that when $\mu a = 0$, i.e., no shield, the heat generation rate becomes

$$H = \frac{\mu_e k \phi_n'(0) \Sigma_a \eta E_\gamma e^{-\mu_t t}}{2\rho \mathcal{K}_t} \left\{ \frac{1}{\mu_t t + f_o(\mu_t t)} - \frac{1}{(1-\beta)\mu_t t + f_o[(1-\beta)\mu_t t]} \right.$$

$$+ \frac{\beta}{\beta - 1} \left[C_1 + C_2 \left(\mu_t t + \frac{\beta - 2}{\beta - 1} \right) \right]$$

$$\left. + e^{(1-\beta)\mu_t t} \left[\ln \left| \frac{1}{1-\beta} \right| - \frac{\beta}{\beta - 1} \left(C_1 + C_2 \frac{\beta - 2}{\beta - 1} \right) \right] \right\} . \qquad \ldots(24)$$

In order to obtain the total contribution from the shield capture gamma rays at a given target position, it is necessary to add to the values obtained from Eq. (23) and (24) the contribution from source regions located in the shield behind the target. Because the above equations hold equally well for $\mathcal{K}_t$ either positive or negative, this additional contribution may be evaluated by using the appropriate values and sign for $\mathcal{K}_t$. Thus, by the use of Eq. (23) and (24), it was possible to evaluate the total shield capture gamma-ray heat generation rate in the target materials positioned at several locations in the water shield.

C. TARGET CAPTURE GAMMA RAYS

The gamma-ray heating in the target samples resulting from thermal neutron capture in the targets was calculated from an expression derived by Storm, et al.[27] The method is based upon a straight ahead scattering approximation for an infinite cylinder containing a uniform isotropic source distribution. Local perturbation of the thermal neutron flux in the vicinity of the target material was not considered. The thermal neutron capture gamma-ray spectra[14,15,16,17] used for the three target materials are given in Table II.

TABLE II

CAPTURE GAMMA-RAY SPECTRA USED FOR TARGET MATERIALS

Aluminum[14, 17]		Iron[16]		Lead[15]	
E_γ(Mev)	(γ_s'/capture)	E_γ(Mev)	(γ_s'/capture)	E_γ(Mev)	(γ_s'/capture)
7.7	0.40	7.65	0.442	7.38	0.93
6.0	0.16	6.00	0.110	6.73	0.07
4.0	0.55	4.20	0.069	-	-
2.6	0.54	2.50	0.68*	-	-
1.0	0.10	1.00	1.70*	-	-

* Assumed contribution

The spectra from iron and aluminum have been simplified in order to reduce the calculational effort. A finer division of the energy groups for the aluminum spectrum was not felt justified because of the relatively small contribution made to the total heat generation rate in this material from the target (n,γ) reaction (see Fig. 6). A finer breakdown of the iron spectrum was not used because detailed information on the energy spectrum in the region below 3.4 Mev was not available. Because the total capture gamma-ray energy released by iron (as accounted for by Kinsey[16]) is 4.3 Mev, all of which is produced above 3.4 Mev, and because the neutron binding energy of the iron nucleus is 7.7 Mev, the additional energy was assumed to be released in the range below 3.4 Mev. In this energy range, two lines were assumed, a 2.5 Mev gamma, 0.68 being produced per capture, and a 1.0 Mev gamma, 1.70 being produced per capture. Using this partially assumed spectrum (see Table II), it was found that the contribution from the 2 lines assumed to exist below 3.4 Mev was approximately 20 per cent greater than that caused by the higher energy radiations.

D. TARGET DECAY BETA PARTICLES

The only significant beta particle given off by any of the target materials is the 2.87 Mev beta resulting from the decay of Al^{28} (Ref. 18). The beta particle disintegration rate was based upon an assumed two-minute irradiation time for the sample. This results in an aluminum activity which is equal to approximately 46 per cent of the saturation activity. Saturation was not assumed here, contrary to the assumption made for the core aluminum, because the aluminum target was subject to activation only during the time that the measurements were being made. The beta energy produced was assumed to be entirely absorbed within the target.

VII. ABSORPTION COEFFICIENTS AND BUILDUP FACTORS

In order to proceed with the calculations, it was necessary to determine the linear absorption coefficients (less coherent scattering) and the energy absorption buildup factors for the core and water shield as well as the energy mass absorption coefficients for the target materials. Values for the linear absorption coefficient and buildup factor for water and the energy mass absorption coefficients for the target materials were obtained from the literature.[11,28,29]

In computing the buildup factor for the core, the "effective Z" method suggested by Goldstein and Wilkins[28] was used. In this method the absorption coefficient per electron(μ_e) for a homogeneous mixture is defined by

$$\mu_e = \sum_i \beta_i \mu_i \quad , \qquad \ldots(25)$$

where μ_i is the corresponding electron absorption coefficient (less coherent scattering) for the i^{th} element in the mixture and β_i is the electron fraction, given by

$$\beta_i = \frac{a_i z_i}{A_i} \Big/ \sum_j \frac{a_j z_j}{A_j} \quad . \qquad \ldots(26)$$

Here, a_i is the weight fraction, A_i the atomic weight, and z_i the number of electrons per atom.

The weight fractions and electron fractions for the core composition listed in Section IV are:

Element	Weight Fraction (a_i)	Electron Fraction (β_i)
hydrogen	0.0381	0.0749
oxygen	0.3020	0.2991
aluminum	0.6375	0.6086
uranium	0.0224	0.0174

The values for the absorption coefficient per electron in the core, calculated from Eq. (25), are plotted in Fig. 4. The shape of this curve was then compared with those of the single elements with the result that for energies above 2 Mev the curve could best be represented by the element for which $Z = 13$, aluminum, and for energies below 2 Mev by the element for which $Z = 26$, iron. Consequently, the aluminum buildup factor was used to represent the buildup factor for the core in calculations involving source energies in excess of 2 Mev, whereas the buildup factor for iron was used in calculations involving energies below 2 Mev.*

The values of the constants A and α, necessary for the evaluation of Eq. (14), were determined from semi-logarithmic plots of the energy absorption buildup factors for iron and aluminum. The energy absorption buildup factor for the 2.23 Mev water capture gamma-ray, as a function of penetration in water, was fitted to a quadratic and the constants C_1 and C_2, necessary for the evaluation of Eq. (23) and (24), were found to be 0.300 and 0.0309, respectively.

The values of μ_s to be substituted into Eq. (14) were obtained by using the relation

$$\mu_s = \rho_s \sum_i \left(\frac{\mu}{\rho}\right)_i a_i \quad , \qquad \ldots(27)$$

* Further theoretical consideration reveals that the aluminum buildup factor should be used for all source energies involved. The error introduced is probably quite small.

where ρ_s is the average density of the core, equal to 1.734 gm/cc and $\left(\frac{\mu}{\rho}\right)_i$ is the mass absorption coefficient (less coherent scattering) of the i^{th} element, in cm^2/gm. A curve of μ_s as a function of gamma-ray energy is plotted in Fig. 5.

VIII. RESULTS

Using the data and the methods described in the previous sections, the heat generation rates in the aluminum, iron, and lead targets were evaluated as a function of distance from the BSR core. The results of these calculations, along with the experimentally measured values, are plotted in Fig. 6, 7 and 8. The experimental values and total calculated values are given in Table III.

A discussion of many of the assumptions made in performing this analysis and their corresponding effect upon the results has been given for similar analyses elsewhere,[2,4] and consequently, will not be repeated here. However, it might be well to summarize briefly some of the more important assumptions used. These are:

a) the power distribution in the core is uniform,

b) the "effective z" method is adequate for determining the effective buildup factor for the core,

c) for the three target materials, the core buildup factor can be used to calculate the heat generation rate as a function of position in the shield,

d) the missing energy in the reported[16] Fe(n, γ) spectrum can be approximated by two low energy lines, a 2.5 Mev gamma and a 1.0 Mev gamma (see Table II),

e) the aluminum target was irradiated for two minutes, resulting in an induced activity approximately 46 per cent of the saturation value, prior to taking the experimental data,

f) the method outlined in WAPD-TN-508[21] for calculating the gamma flux from a finite cylindrical source of uniform source intensity can be used to evaluate heat generation rates in the targets resulting from core gammas.

On the basis of the results shown in Fig. 6, 7, and 8, and in Table III, these assumptions appear to have been quite reasonable for this analysis.

TABLE III

CALCULATED AND MEASURED HEAT GENERATION RATES

Distance From Core Face (in.)	Heat Generation (watts/gm-Mw)					
	Core Gammas	Water Capture Gammas	Target Capture Gammas	Target Decay Betas	Calculated Total	Experimental Total
Aluminum						
0	0.1831	0.0181	0.0031	0.0277	0.2320	-
0.5	0.1530	0.0210	0.0037	0.0340	0.2117	0.219
2.0	0.0952	0.0208	0.0029	0.0265	0.1454	0.132
4.0	0.0555	0.0142	0.0012	0.0109	0.0818	0.0745
9.0	0.0187	0.0053	0.0001	0.0007	0.0248	-
Iron						
0	0.2190	0.0179	0.0530	-	0.2899	-
0.5	0.1720	0.0208	0.0641	-	0.2569	0.271
2.0	0.0971	0.0205	0.0516	-	0.1692	0.173
4.0	0.0552	0.0140	0.0210	-	0.0902	0.105
9.0	0.0186	0.0052	0.0014	-	0.0252	-
Lead						
0	0.4490	0.0198	0.0014	-	0.4702	-
0.5	0.3618	0.0232	0.0017	-	0.3867	0.332
3.0	0.1486	0.0196	0.0009	-	0.1691	0.175
4.0	0.1095	0.0159	0.0005	-	0.1259	-
6.0	0.0644	0.0106	0.0002	-	0.0752	0.090
9.0	0.0326	0.0058	0.00004	-	0.0384	0.043

IX. CONCLUSIONS

Because of the small discrepancies between the calculated and measured heat generation rates in the target materials, it is not felt that additional refinements in the methods described here can be justified. With the development of improved techniques for handling gamma-ray buildup in heterogeneous media and for determining thermal neutron flux distributions in reactor shield regions, considerable improvement in calculational accuracy may be obtained both for simple shields, as was the case in this analysis, and for shields of considerable complexity. However, because of the excellent agreement between experimental and calculated values, it is concluded that the basic gamma-ray data and calculational methods employed may be used in similar analyses for other reactor systems.

REFERENCES

1. F. T. Binford, E. S. Bettis and J. T. Howe, "Gamma Heating Measurements in the Bulk Shielding Reactor," ORNL-CF-56-3-72, March 7, 1956.

2. R. L. Ashley and D. S. Duncan, "The Theoretical Calculation of the Attenuation of Gamma Radiation From a Swimming Pool Type Reactor," NAA-SR-1921, August 15, 1957.

3. W. M. Breazeale, "The New Bulk Shielding Facility at Oak Ridge National Laboratory," ORNL-991, May 8, 1951.

4. H. W. Bertini, C. M. Copenhaver, H. C. Claiborne and T. Fowler, "Comparison of Calculated vs Measured Gamma-Ray Heating in the Bulk Shielding Facility," CF-56-11-36, Nov. 12, 1956. Also, Nucleonics 15, Oct., 1957.

5. H. W. Bertini, C. M. Copenhaver, A. M. Perry, and R. B. Stevenson, ORNL-2113, October 3, 1956, Classified.

6. B. B. Kinsey, R. C. Hanna, and D. Van Patter, "Gamma-Rays Produced in the Fission of U^{235}," Canadian Journal of Research 26A, 79-98 (1948).

7. M. Deutsch and H. Rotblat, "Investigation of Fission Gamma-Rays," AECD-3179, Nov. 13, 1944.

8. F. C. Maienschein and R. C. Cochran, "Prompt Fission Gamma-Rays," Paper Presented at the Reactor Shielding Information Meeting, Chicago, Ill., Nov. 12-13, 1953.

9. R. L. Gamble, "Prompt Fission Gamma-Rays from Uranium 235," Reactor Shielding Information Meeting, May 12-13, 1955, Engineer Research and Development Laboratories, Fort Belvoir, Virginia, WASH-292 (Pt. 3), September, 1955, p. 28-31.

10. F. C. Maienschein, "Table of Current Values for the Distribution of Energy Released by the Fission of U^{235} Induced by Thermal Neutrons," CF-58-4-25, April 7, 1958.

11. "The Reactor Handbook, Vol. I. Physics", AECD-3645, March 1955.

12. D. J. Hughes and J. A. Harvey, "Heavy Element Cross Sections Presented at Geneva, August, 1955," Addendum to BNL-325, July 15, 1955.

13. R. E. Bell and L. G. Elliott, "Gamma-Rays from the Reaction $H^1(n,\gamma)D^2$ and the Binding Energy of the Deuteron," Phys. Rev. 79, 282-85 (1950).

14. B. B. Kinsey, G. A. Bartholomew, and W. H. Walker, "Neutron Capture Gamma Rays From Fluorine, Sodium, Magnesium, Aluminum, and Silicon," Phys. Rev. 83, 519-534 (1951).

REFERENCES (Continued)

15. B. B. Kinsey et al., "Neutron Capture Gamma-Rays from Lead and Bismuth," Phys. Rev. 82, 380-388 (1950).

16. B. B. Kinsey et al., "Neutron Capture Gamma-Rays from Titanium, Chromium, Iron, Nickel, and Zinc," Phys. Rev. 89, 375 (1953).

17. T. H. Braid, "Neutron Capture Gamma-Rays From Various Elements," Phys. Rev. 102, 1109-1123 (1956).

18. J. M. Hollander, I. Perlman, and G. T. Seaborg, "Table of Isotopes," Rev. Mod. Phys. 25, 469-651 (April, 1953).

19. R. W. Peele, W. Zobel, and T. A. Love, "Measurement of the Spectrum of Short-Lived Fission-Product Decay Gamma Rays Emitted from a Rotating Fuel Belt," ANP Division Annual Report for Period Ending Sept. 10, 1956, ORNL-2081, p. 91-101.

20. K. Way, E. P. Wigner, "Radiation From Fission Products," MDDC-48 (June 14, 1946).

21. A. Foderaro and F. E. Obenshain, "Fluxes From Regular Geometric Sources," WAPD-TN-508, June, 1955.

22. J. J. Taylor and F. E. Obenshain, "Flux From Homogeneous Cylinders Containing Uniform Source Distributions," WAPD-RM-213, Dec. 7, 1953.

23. Samuel Glasstone, Principles of Nuclear Reactor Engineering, p. 593, (Van Nostrand, New York, 1955).

24. F. C. Maienschein, et al., "Attenuation by Water of Radiations From a Swimming Pool Type Reactor," ORNL-1891, Sept. 19, 1955.

25. Personnel Communication, K. M. Henry and E. B. Johnson, Oak Ridge National Laboratory.

26. A. R. Vernon, "Analysis of the Biological Shield of the Sodium Reactor Experiment," NAA-SR-1949, June 15, 1957.

27. M. L. Storm, H. Hurwitz, Jr., and G. M. Roe, "Gamma-Ray Absorption Distributions for Plane, Spherical, and Cylindrical Geometries," KAPL-783, July 24, 1952, Classified.

28. Herbert Goldstein and J. Ernest Wilkins, Jr., "Calculations of the Penetrations of Gamma Rays," NYO-3075, June 30, 1954.

29. Gladys R. White, "X-Ray Attenuation Coefficients From 10 Kev to 100 Mev," NBS-1003, May 13, 1952.

30. R. L. French, "Reactor Shield Heating Calculations for Gamma Rays," Paper presented before American Nuclear Society (Los Angeles, June 2-4, 1958).

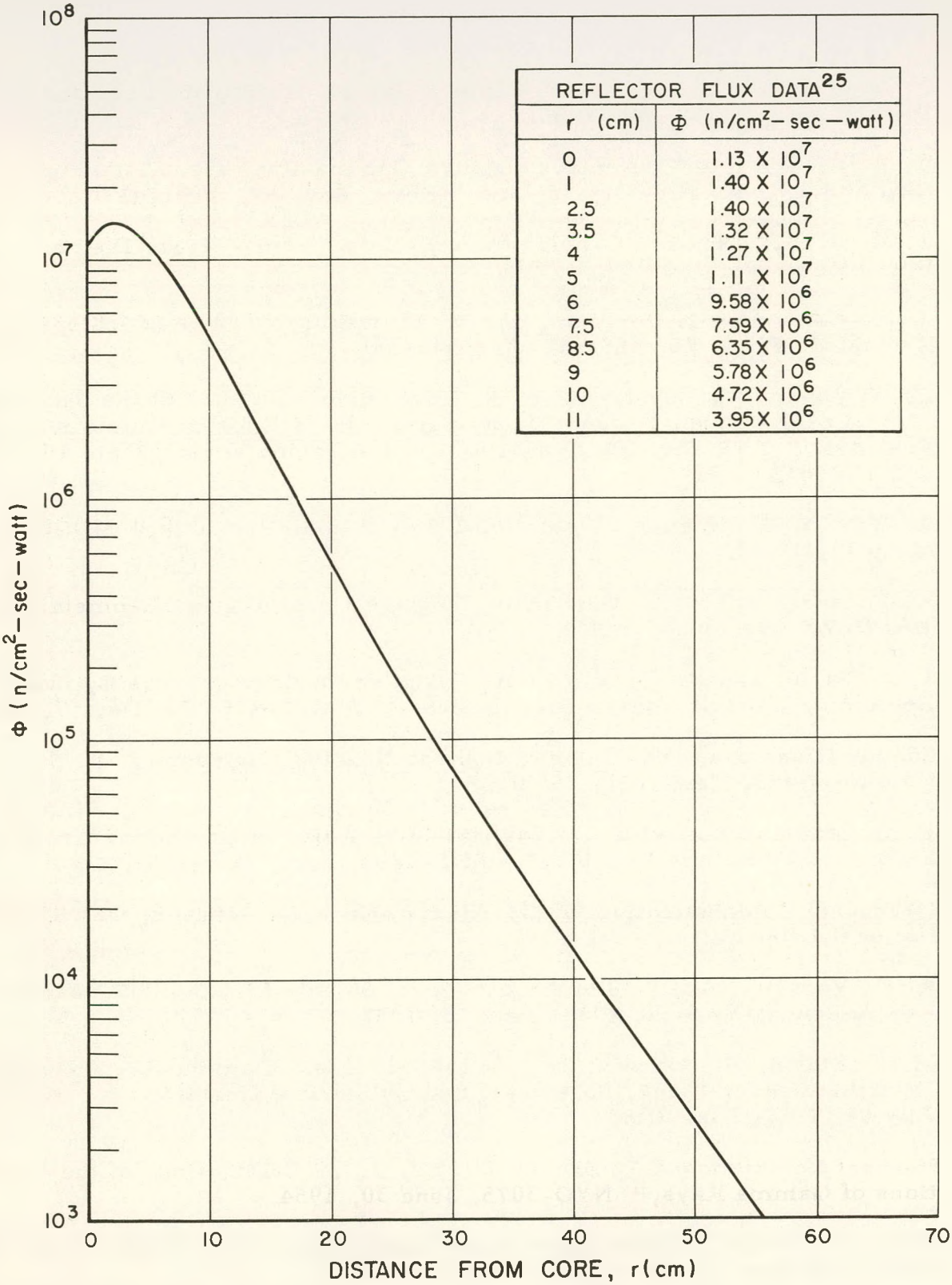

Fig. 1. Thermal Neutron Flux in BSR Water Shield for Loading 33

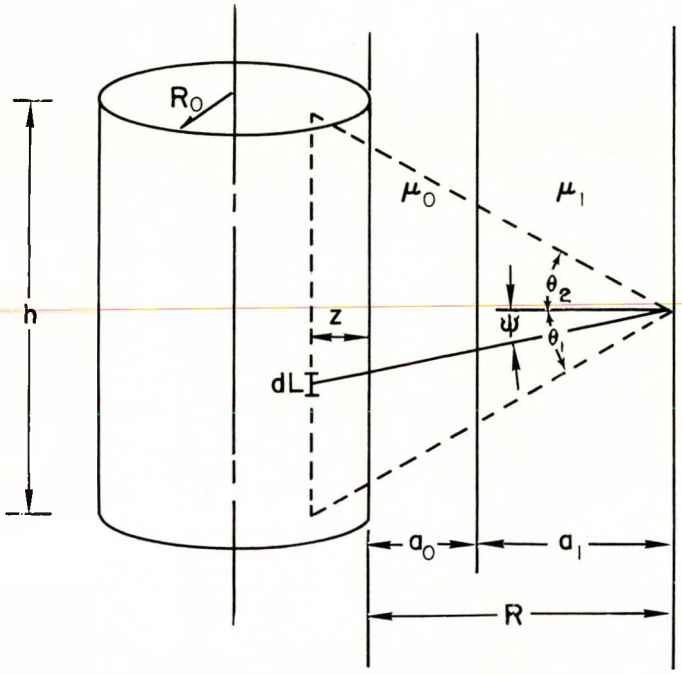

Fig. 2. Geometry for Uniform Cylindrical Source With Slab Shield

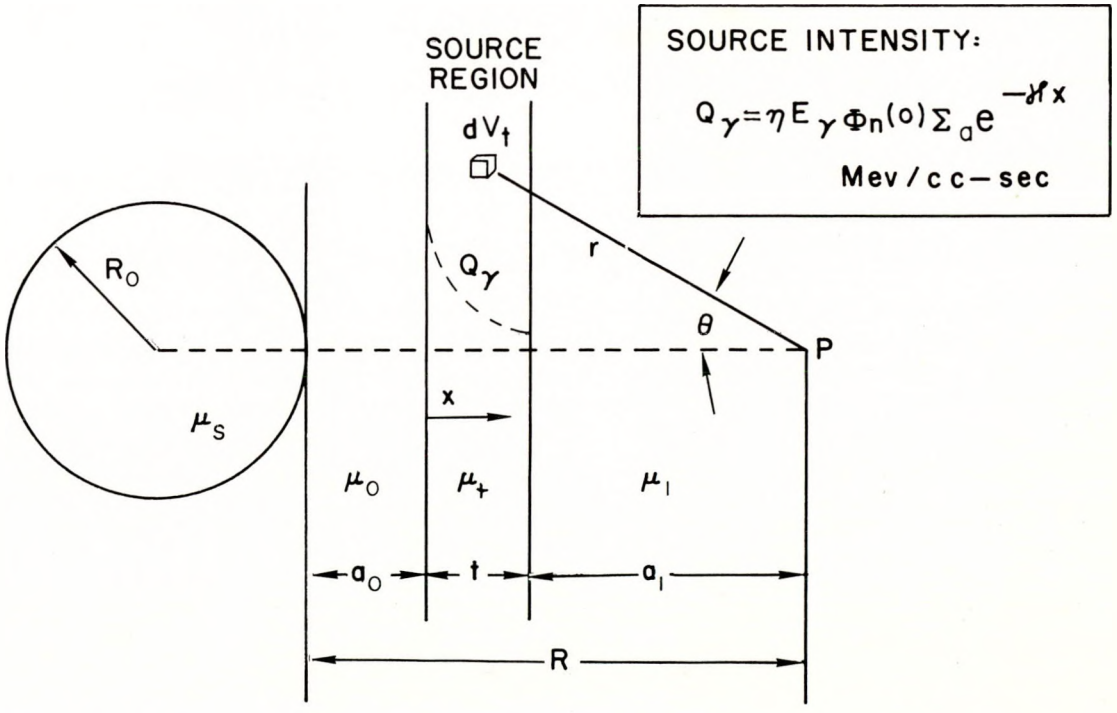

Fig. 3. Geometry for Exponential Slab Source with Slab Shield

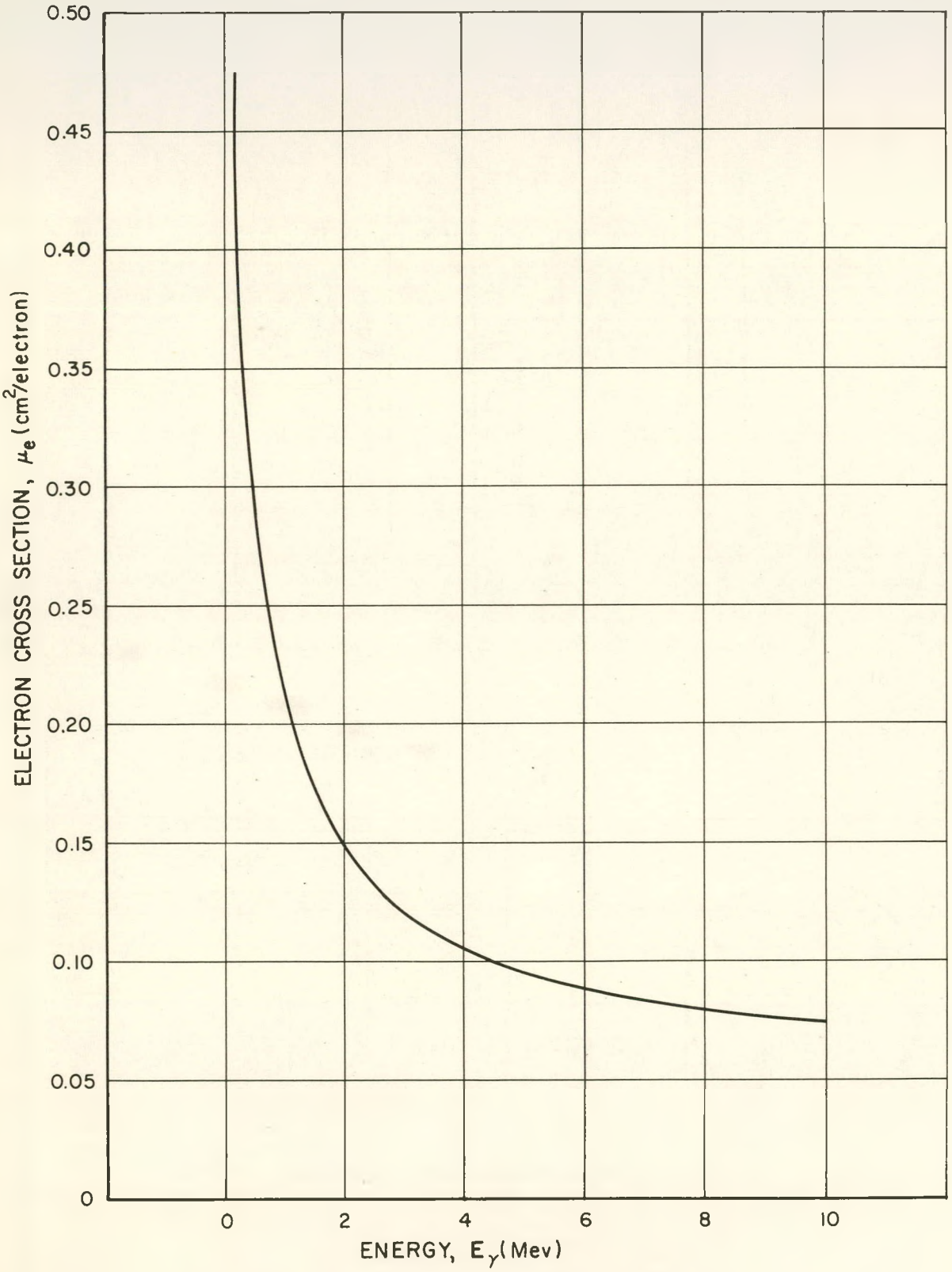

Fig. 4. Electron Cross Section for BSR Core

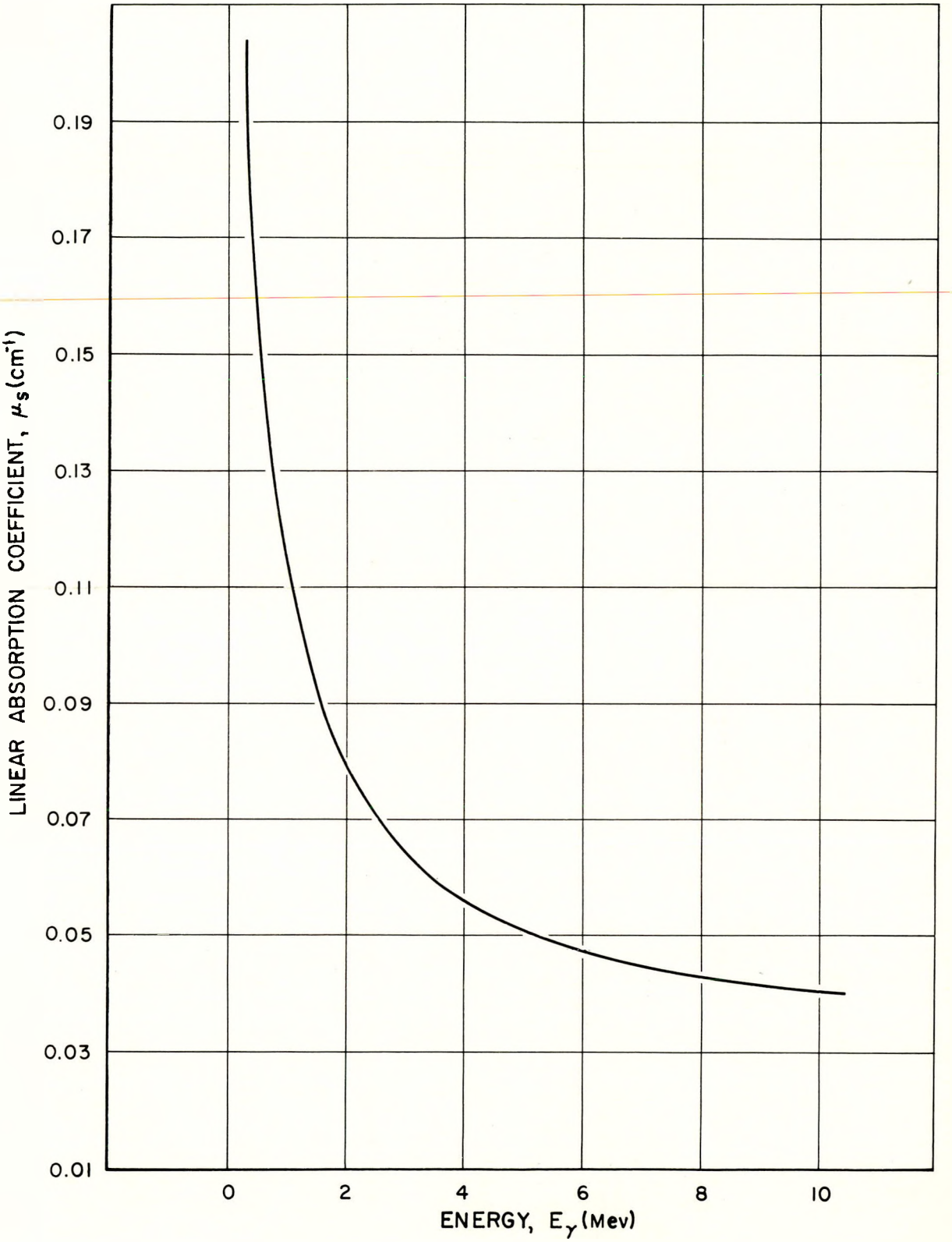

Fig. 5. Linear Absorption Coefficient for BSR Core

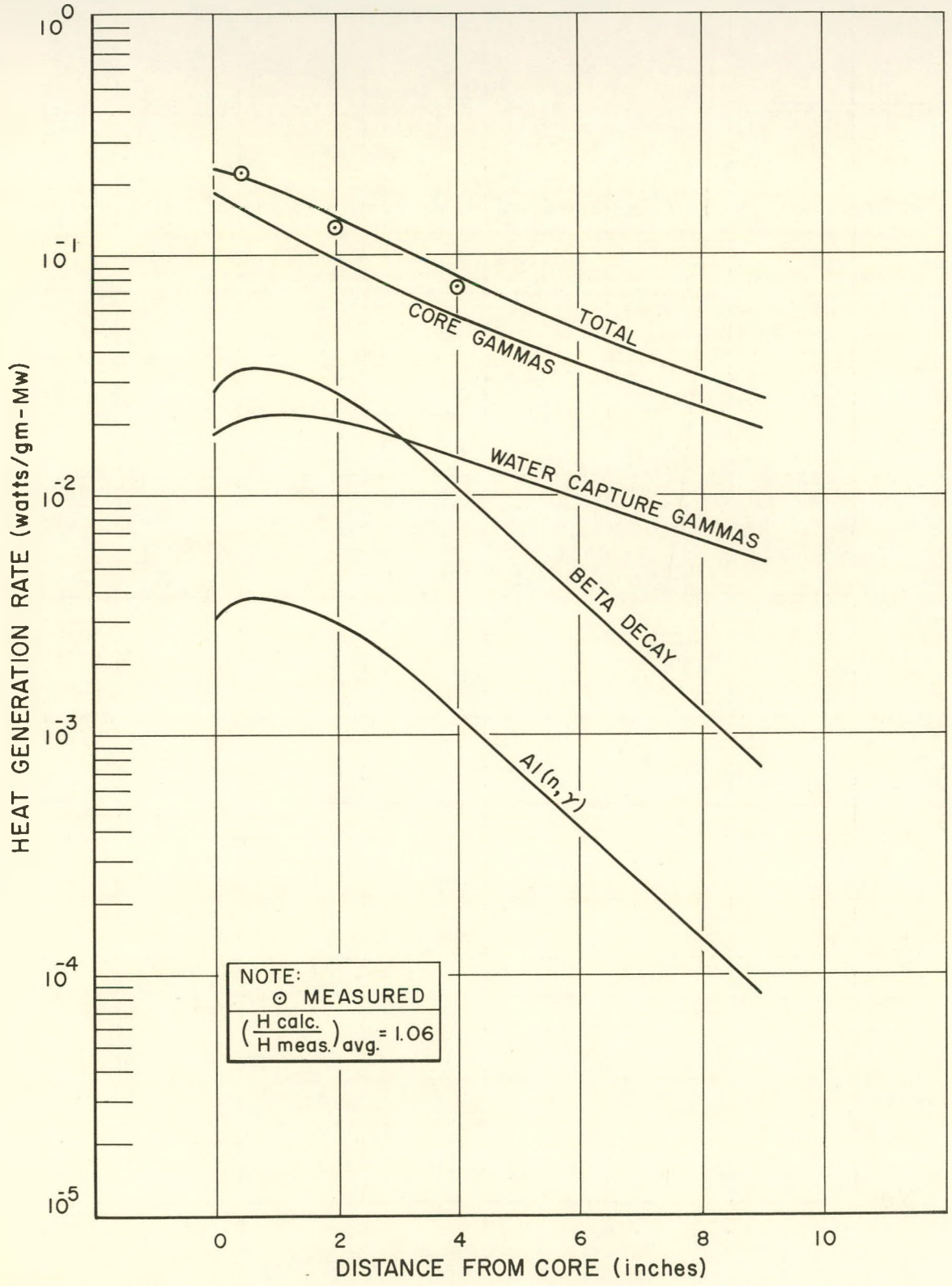

Fig. 6. Gamma-Ray Heating in Aluminum Target

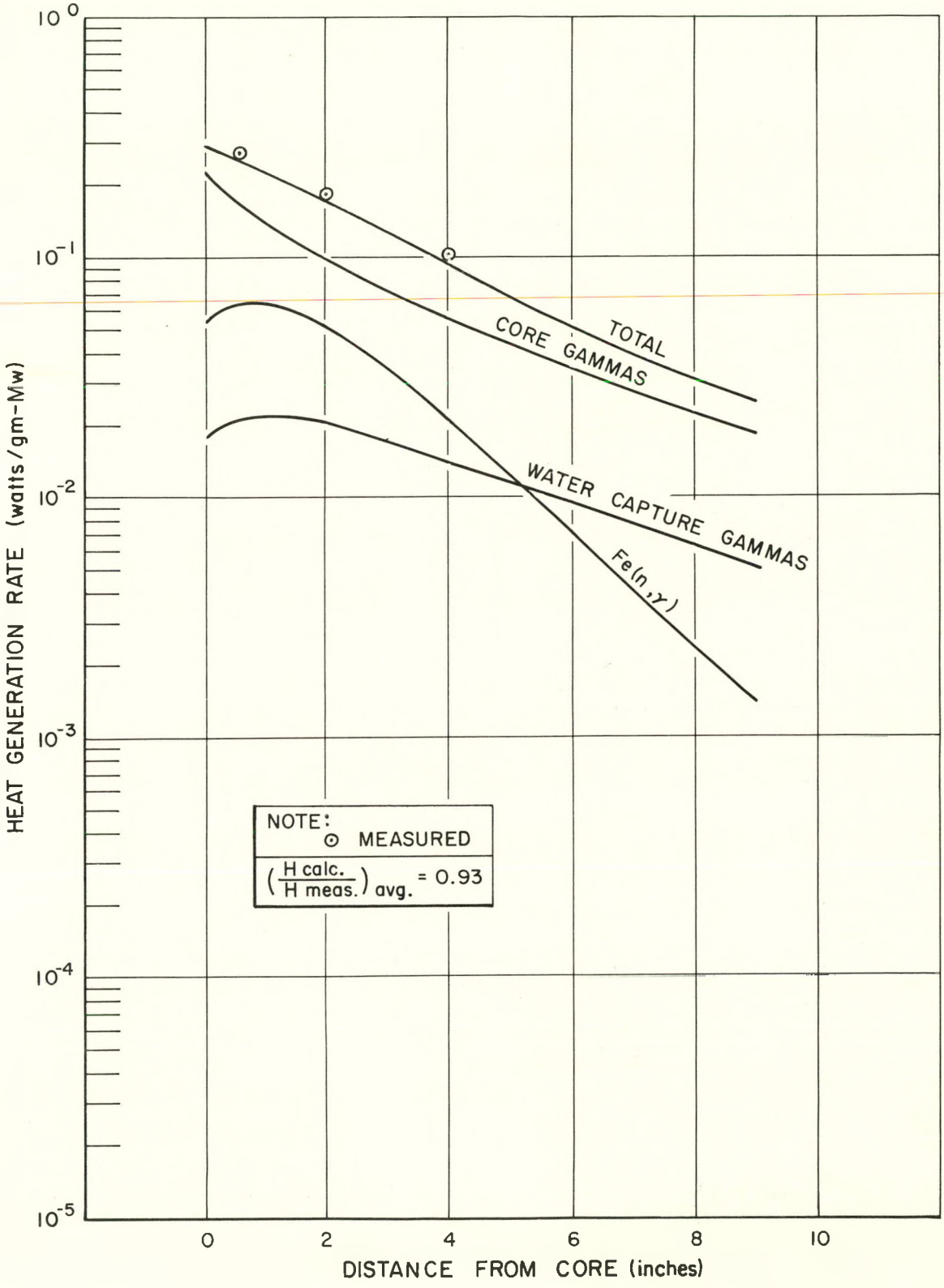

Fig. 7. Gamma-Ray Heating in Iron Target

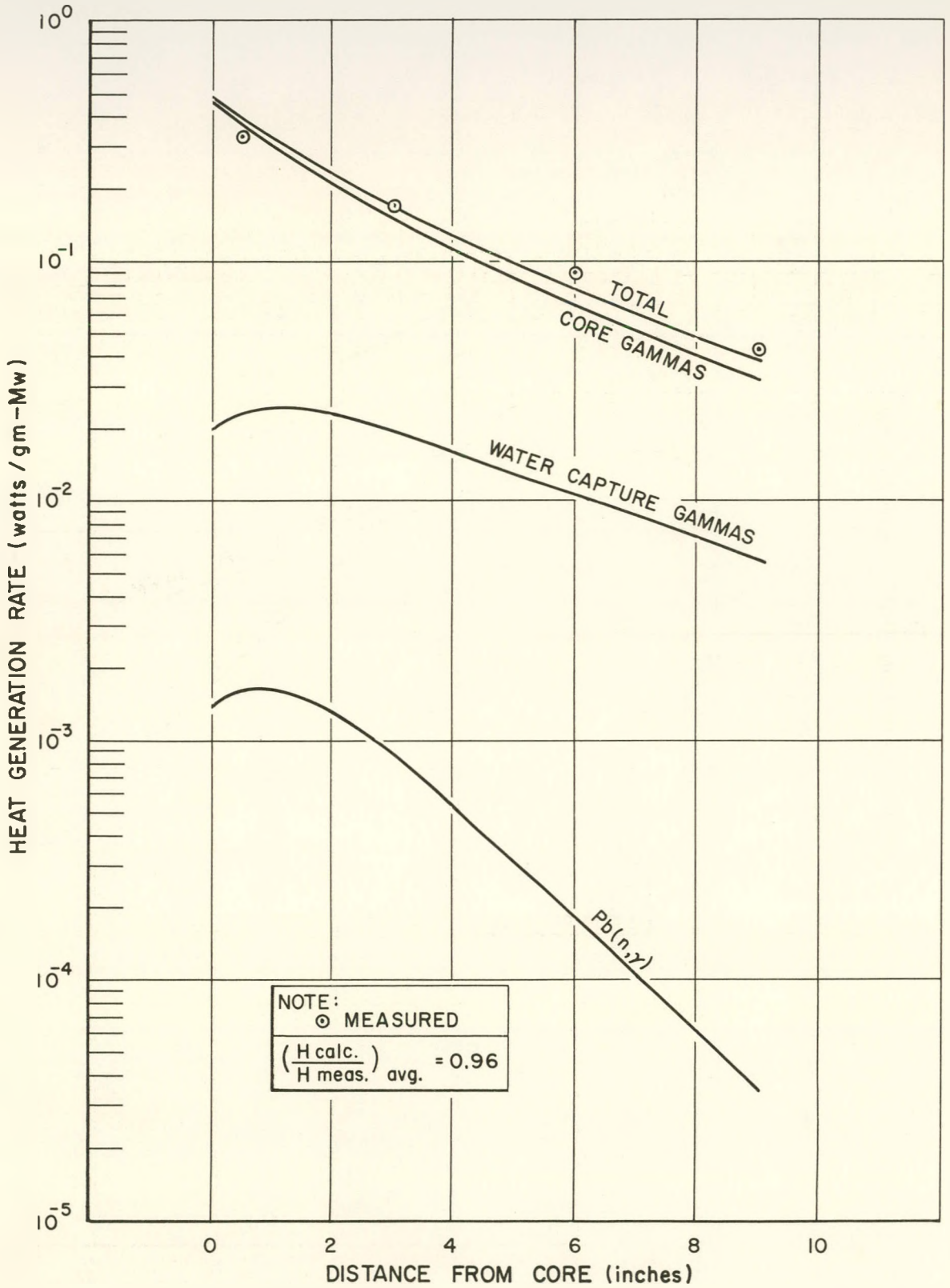

Fig. 8. Gamma-Ray Heating in Lead Target